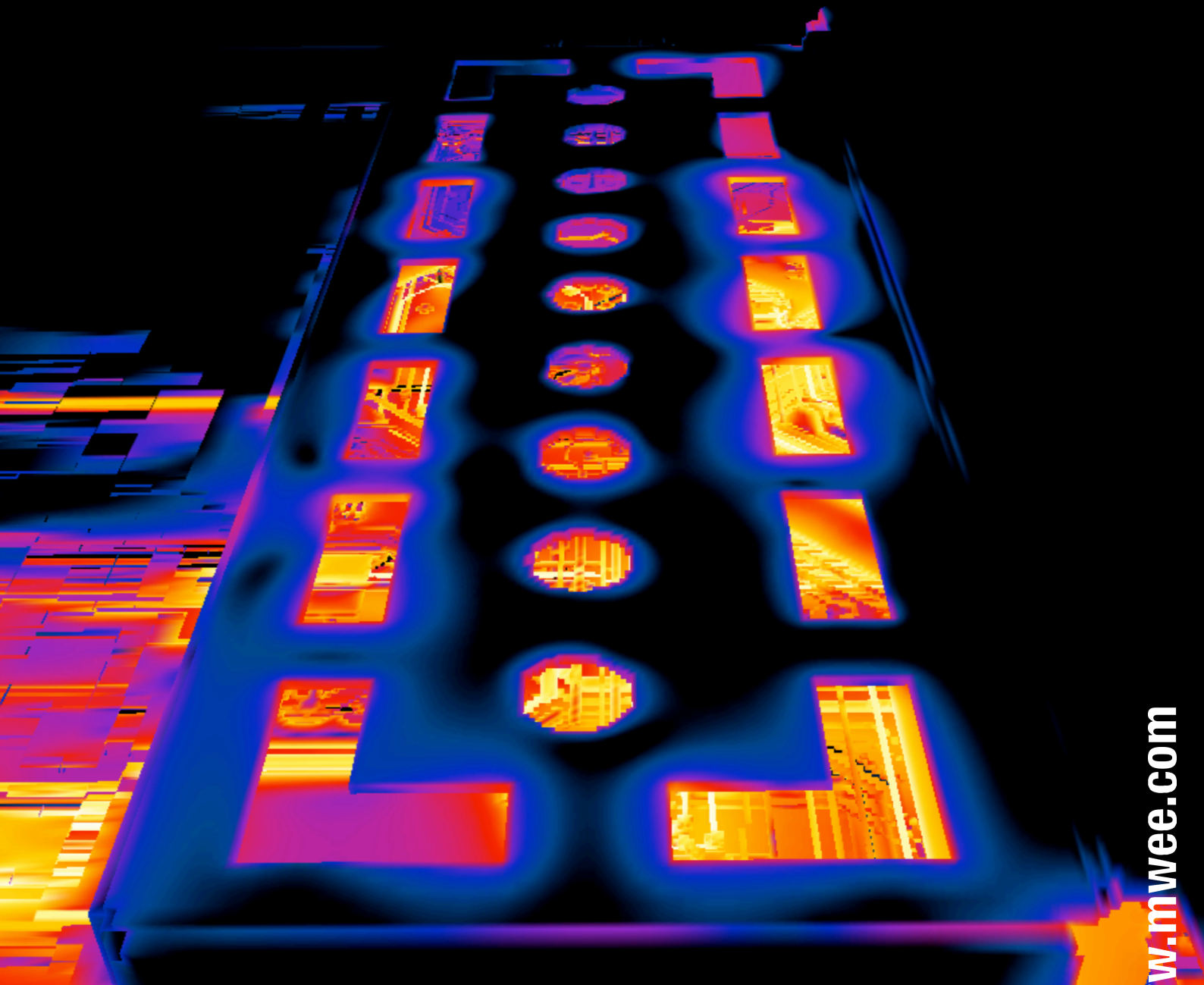


July/August 2009

United Business Media

MICROWAVE ENGINEERING

EUROPE



Advances in CAD/EDA

CMOS & RF technology

Cover feature: tracing route - latest EDA tools conquering today's EMI challenges

www.mw.com

The European journal for the microwave and wireless design engineer

BPA
WORLDWIDE
BUSINESS

Effective full 3D EMI analysis of complex PCBs by utilizing the latest advances in numerical methods combined with novel time-domain measurement technologies.

By Chung-Huan Li, Peter Futter, Nicolas Chavannes, and Niels Kuster

I. Introduction

In the past, there was limited use of numerical electromagnetic analysis to analyze EMI issues on PCB, especially for complex boards with both high performance digital and RF components. While 2.5-D solvers and additional approximations may have been sufficient in the past, complex PCBs require full-wave 3-D analysis to accurately capture complex field interactions. The latest advances in FDTD methods offer several advantages for addressing and solving these challenges, including computational requirements, time- and frequency-domain results and a straightforward real-time meshing approaches. The FDTD method also inherently lends itself to affordable GPU based hardware acceleration solutions. Simultaneously, significant advances in sensor technology combined with the latest advances in FDTD methods promises routine comprehensive analysis of complex PCM or multi-chip modules.

II. PCB-level EMC/EMI problem outline

Setup and methods

The PCB platform, the analysis of which is described in this short article, was developed by a leading technology company for integration into a candy bar type mobile phone. The results were obtained in a joint project between Schmid & Partner Engineering AG, SPEAG [1] and the technology partner.

A) *Simulation Platform SEMCAD X*: The simulation platform SEMCAD X V13.4 [2] and a CIB1000 were applied

for all implementations and assessments. SEMCAD X is a universal simulation platform with a high-end ACIS® based modeler CAD importer and graphical user interface (in-house 3-D OpenGL renderer) that integrates various solvers providing native 64 bit functionality, such as full-wave EM solvers (FIT/C-FDTD, C-ADI-FDTD, etc.), FEM based low frequency and static solvers, thermal solvers for thin conductors, vessel trees, coupled full-wave EM-SPICE circuit solvers and a GA based optimization platform.

By combining SEMCAD X with Acceleware's [4] latest Nvidia GPU CUDA based high performance systems, e.g. the ClusterInABox (CIB), simulations can be performed hundreds of times faster than on a common desktop multi-processor machine. A post-processing engine and Python scripting allowed for result extraction/visualization (time- and frequency-domain, near-/far-field) and general automation. The combined platforms, DASY5 and SEMCAD X directly compared the numerical and experimental data.

B) *Novel Time Domain Sensor*: A novel time-domain H-field sensor has been developed to perform PCB and chip-level scans of the emitted H-fields from integrated circuits. The sensor is based on electro-optical technologies providing extremely high sensitivity without perturbing the near-fields over the IC through optically de-coupled power supply and data transmission. The sensor provides a sensitivity of better than $-120 \text{ dB}((\text{A/m})/(\sqrt{\text{Hz}}))$ over a wide frequency range from 500 MHz to 6 GHz. The sensor

can be fully integrated into the DASY5 NEO scanning system. In addition to the standard user interface for EMC analysis, a novel Python based scripting interface provides the user with the ability to adapt the software to rapidly changing requirements. The results from the IC scans can be directly displayed in SEMCAD X (see Figure 1).

Goals

Multiple goals were defined for the project:

- 1) reproduce the known RF performance of the PCB platform with the numerical model
- 2) study and understand the board level coupling mechanisms at various locations
- 3) apply this knowledge to optimize the shielding
- 4) highlight the benefits of applying high performance FDTD based simulation toolkits, like SEMCAD X, for typical board level EMC and EMI problems.
- 5) validate by measurements

Configuration

The CAD model of the PCB was originally imported as a .SAT file. A fully featured ODB++ interface [5] was integrated into SEMCAD X to directly import complex hierarchical PCB layout structures. The stackup for this investigation consisted of 4 layers, dielectric substrates and via interconnects.

The model of the full PCB layout including the antenna is shown in Figure 2. Figures 3 and 4

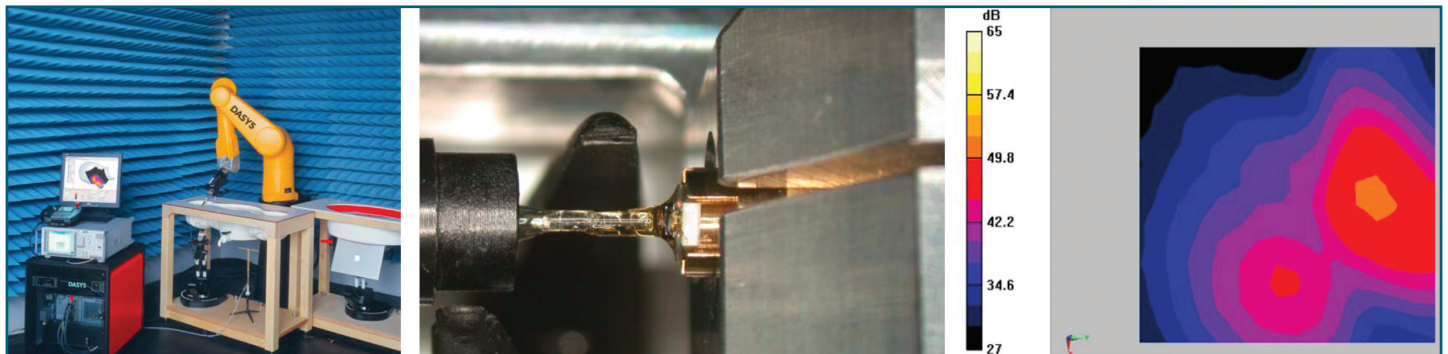


Figure 1: The DASY5 scanner (left), a close-up of the sensor probe tip of the H-field time-domain sensor where the diameter of the loop is 2.6 mm (middle), and the H-field measurement results of a scan above an IC exported from SEMCAD X (right).

highlight the main region of interest on the board, the 16 active Traffic traces below the shielding. The Traffic traces are fed independently by 16 voltage sources (source region) in the FDTD simulation. Each Traffic trace is connected at two locations to the system ground with a 27 pF capacitor (capacitor regions). 3 Victim ports are defined on the board as shown in Figure 3: Victim 1 is the antenna feedpoint, Victim 2 and Victim 3 are defined at either end of the Victim trace. Victim 2 is located outside the shielding area and Victim 3 is located underneath the shielded region (see also Figure 5). All three victims are defined as 50 Ohm ports within the simulation.

Three scenarios for different shieldings, full shielding, hole shielding and no shielding, were investigated, as described in Figure 5.

The simulations were conducted in less than 12 hours (simulation speed: > 350 MCells/s) using the CIB1000 accelerator. The simulations were finalized in less than 3 hours (speed: 1500 MCells/s) with the latest generation of NVidia GPU and SEMCAD X's CUDA based implementation.

For the purpose of this study, a relative isolation parameter was defined to investigate the coupling between the Traffic and Victim traces:

Figure 2: The development phone PCB model used in this study, PCB (left) and detailed trace view (right).

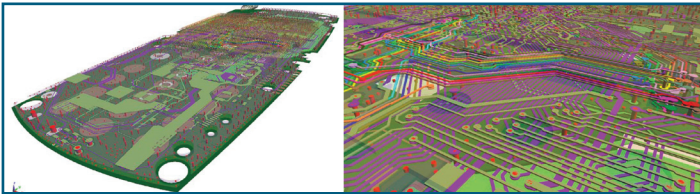


Figure 3: The layout of the active 16 Traffic traces, the 3 Victim ports and the Victim trace.

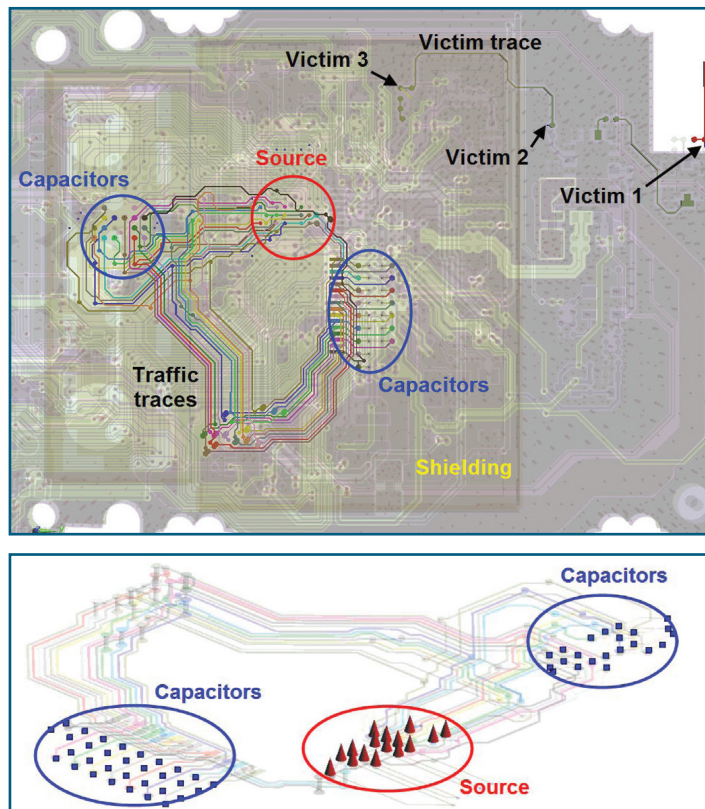


Figure 4: The 16 Traffic traces on the PCB; the blue points and red arrows are the locations for capacitors and sources, respectively.

$$\text{Isolation (dB)} = 10 \cdot \log(P_{v,k} / P_{in}), k = 1, 2, 3 \quad (1)$$

where $P_{v,k}$ is the real part of the power received at Victim port k and, P_{in} is the summation of the real part of the input power of all 16 Traffic traces.

The relative isolation can be calculated at all 3 Victims from one single broadband FDTD simulation. At least 16 simulations would have to be conducted using a traditional coupling definition.

IV. Simulation results and interpretation

A) Phone PCB

The relative isolation (defined in equation (1)) at Victims 1, 2 and 3 for the 3 different shielding cases is shown in Figure 6. The observed results can be summarized as follows:

Victim 1: both full and hole shielding reduce the isolation compared to no shielding because the shielding suppresses radiation from the Traffic traces.

Victim 2 and 3 have similar isolation for the 2 shielded cases, with the hole shielding offering better isolation than the full shielding (approximately 6 – 8 dB over the frequency band). The isolation, however, differs for the no shielding case. This observation is studied in more detail in the next section (B).

The results in Figure 6 agree well with experimental data obtained by examining the board at 880 MHz.

Figure 7 shows the Poynting vector ($\mathbf{S} = \mathbf{E} \times \mathbf{H}$) distribution in the plane at 1 mm above the PCB, where there is weaker coupling to Victim 3 for the hole shield. The shielding confines the currents from the Traffic traces within the shielded region and thus, predominantly couples to Victim 3 (which in turn couples to Victim 2 through the Victim trace). However, when there is no shielding, the current is no longer confined and couples directly to both Victim 2 and Victim 3 through the whole PCB.

Figure 5: The three shielding configurations: full shielding (left), hole shielding (middle) and no shielding (right).

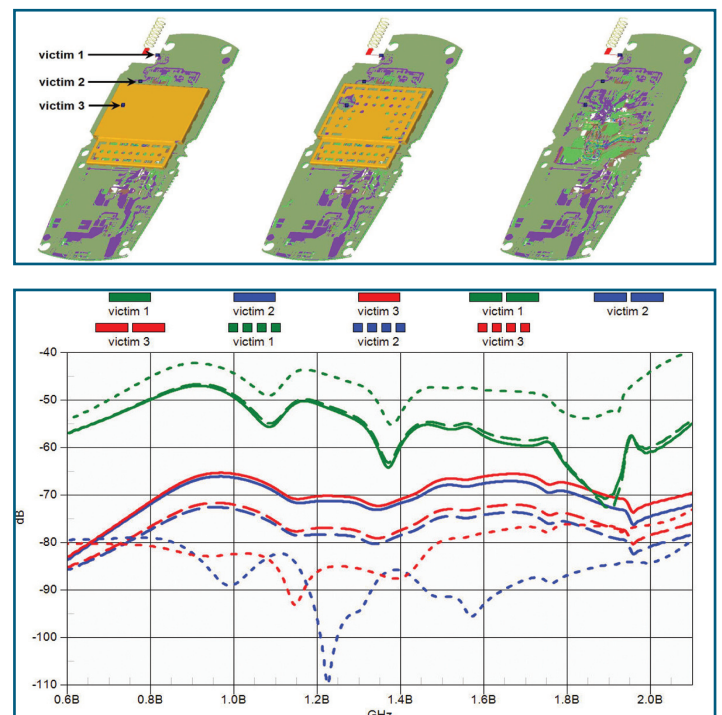


Figure 6: The simulation results addressing isolation for the three configurations: full shielding (solid), shielding with holes (dashed) and without shielding (dotted).

Figure 7: The Poynting vector distribution at 880 MHz in a plane at 1 mm above the PCB with full shielding (left) and hole shielding (right).

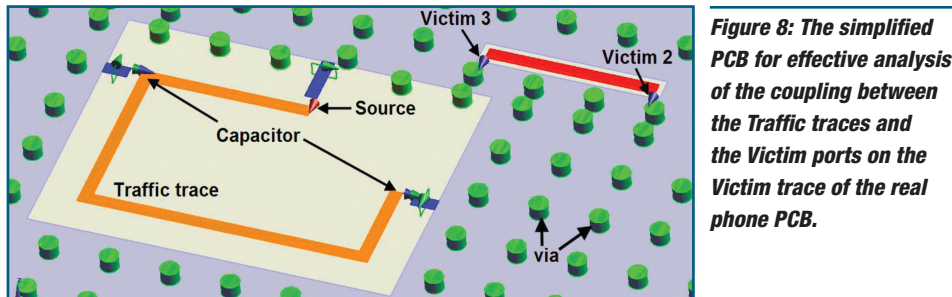
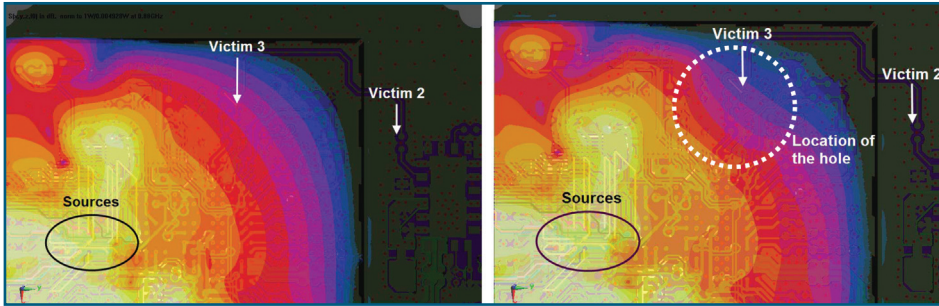
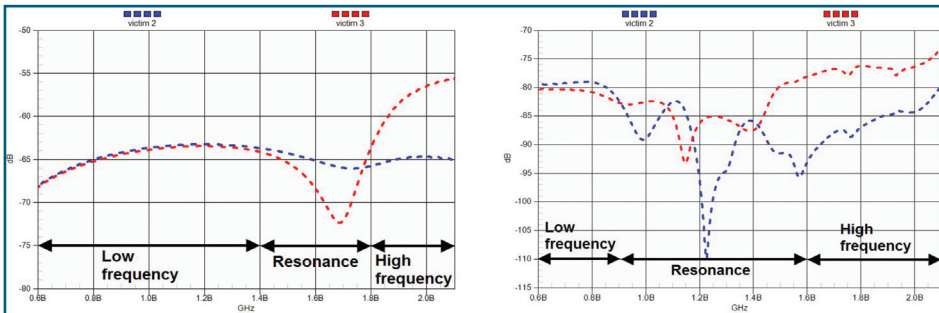


Figure 8: The simplified PCB for effective analysis of the coupling between the Traffic traces and the Victim ports on the Victim trace of the real phone PCB.

Figure 9: Isolation of Victim 2 (blue) and Victim 3 (red) in the simplified model (left) and the real PCB (right).



B)

Figure 10: The transmission line model of the currents flowing on the Victim trace.

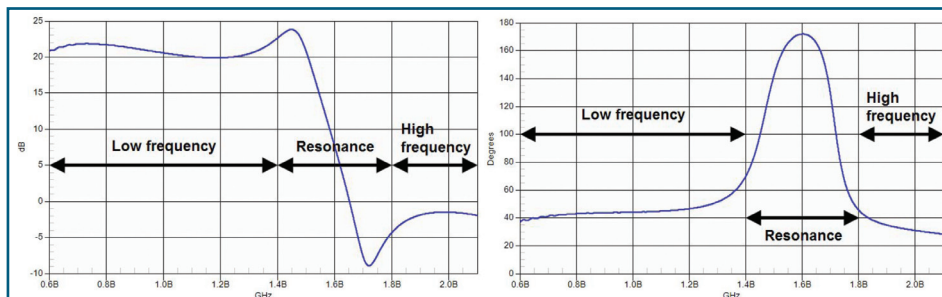
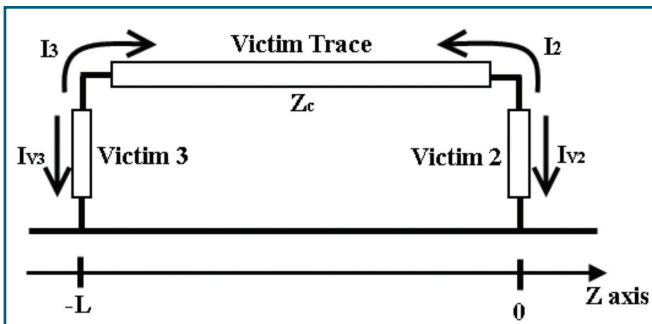


Figure 11: The ratio of the magnitude I_3/I_2 in dB (left) and the phase in degrees (right).

B) Simplified PCB model with no shielding

A simplified PCB model, as depicted in Figure 8, was developed to explain the difference in isolation between Victim 2 and Victim 3 with no shielding. The simplified PCB has only one voltage source and one Traffic trace, and is modeled as infinitely planar extended (terminated with UPML boundaries) to exclude the boundary effects from the PCB. The simplified model can be simulated in a few minutes (geometrical changes can be studied quickly) and it supports a more intuitive analogy to easily describe it in terms of resonance lengths.

Figure 9 shows the level of isolation of the simplified model compared to that of the real PCB. The isolation in the simplified model behaves similarly to that of the real board. The frequency band can now be described as three regions: Low frequency (similar isolation), Resonance (notches in isolation) and High frequency (Victim 3 has weaker isolation).

To further qualify the three regions, a transmission line approach (Figure 10) is used to analyze the current on the Victim trace of the simplified PCB.

The relation between the currents is as follows:

$$\begin{cases} I_{V2} = I_3 - I_2 \\ I_{V3} = I_2 e^{-j\beta L} - I_3 e^{j\beta L} \end{cases} \quad (2)$$

where I_{V2} and I_{V3} are the simulated currents in port Victim 2 and 3, respectively, and can be used to calculate the currents I_2 and I_3 on the Victim trace.

Figure 11 shows the magnitude ratio and the phase difference between I_3 and I_2 . In the low frequency region, since I_3 is much bigger than I_2 , there is only one dominant coupling to the victim trace and the current flows from Victim 3 to Victim 2. Therefore, the isolation of Victim 2 and Victim 3 is very similar in this region. In the resonance region, the resonance of the Traffic trace changes in the isolation differences. I_2 and I_3 have similar magnitudes but different phases in the high frequency region. The difference in phase plus the phase lag caused by the transmission line lead to destructive and constructive isolation on Victim 2 and Victim 3, respectively.

The 16 Traffic trace in the real phone PCB model is responsible for the large number of notches seen in the isolation in the resonance region (Figure 9), resulting in a more complex coupling between the Traffic and Victim trace. The transmission line model describes the fundamental behavior in detail.

Based on the combination of a simplified PCB model with transmission line analysis, the coupling to the Victim trace (and Victim 2 and 3) can also be well quantified for the no shielding case. A thorough understanding of the current flow can subsequently be used to improve the design of the shielding.

V. Validation

The results can be finally validated by the prototype sensor system described above. The system is

outlined in Section II.B) (see Figure 1 for setup and procedure).

VI. Conclusions

A multilayer PCB board developed for a mobile phone by a leading technology company was CAD-imported and numerically assessed using the EM simulation platform SEMCAD X. A detailed characterization of the board level coupling, field distribution and radiation behavior was achieved through comprehensive simulations. The simulation results of the relative isolation recorded at the 3 victim ports agree well with experimental results for the 3 different shielding configurations. Furthermore, a simplified PCB model with transmission line analysis was used to elaborate on the differences observed in specific configurations, namely the Victim 2 and 3 isolations for the no shielding case.

Finally, the study and the quality of the results clearly outline the advantages of integrating high performance EM simulation packages like SEMCAD X into industrial R&D processes on a regular basis. The straightforward application of the presented techniques, namely an easy (e.g., ODB++) import and handling of multiple 10'000 CAD parts, interactive real-time meshing, 3-D full-wave (transient) simulation in time-domain within a few hours only and powerful postprocessing tailored, e.g., specifically for EMI applications, are ideal for addressing today's EMI and EMC challenges on complex PCB. The combination with EM-Spice co-simulation and GA based optimization platforms further enhances the method's capabilities.

SEMCAD X in combination with the smoothly integrated novel time-domain scanner will become the optimal analysis, design and synthesis tool kit for complex PCB and multi-module chips.

VII. Acknowledgements

This study was generously supported by the Swiss Commission for Technology and Innovation (CTI) and assisted by the Foundation for Research on Information Technologies in Society (IT²S), Switzerland.

VIII. References

- [1] Schmid & Partner Engineering AG, www.speag.com.
- [2] SEMCAD X Reference Guide, V13.4, www.semcad.com.
- [3] N. Chavannes et al., "Suitability of FDTD-based TCAD tools RF design of mobile phones, IEEE Antennas and Propagation Magazine, vol. 45, no. 6, pp. 52 – 66, 2003.
- [4] www.acceleware.com.
- [5] <http://www.valor.com/en/Products/ODBpp.aspx>.

